Electronic Supplementary Material (ESI) for Journal of Materials Chemistry C.

Asymmetric Sky-Blue Thermally Activated Delayed Fluorescence Emitters Bearing Tris(triazolo)triazine Moiety for Solution Processable Organic Light-Emitting Diodes

Zhou Fang,[a] Shengyue Wang,[a] Junxu Liao,[b] Xinrui Chen,[a] Yuanyuan Zhu,[a] Weiguo Zhu[a]*, Yafei Wang[a]*

[a]*Jiangsu Collaborative Innovation Center of Photovoltaic Science and Engineering, Jiangsu Engineering Laboratory of Light-Electricity-Heat Energy-Converting Materials and Applications, School of Materials Science & Engineering, Changzhou University, Changzhou 213164, China.*

Email: W. Zhu: zhuwg18@126.com; Y. Wang: qiji830404@hotmail.com

[b]*School of Chemical Engineering and Energy Technology, Dongguan University of Technology, Dongguan, 523808, China*

Contents

Experimental part

All synthetic materials are commercial from Energy Chemical Company Ltd. and used in the reaction directly. All reactions were carried out under N_2 atmosphere.

In order to determine the structure of the compound, ^1H NMR and ^{13}C NMR spectra were acquired using a Bruker Dex-300/400 NMR instrument using $CDCl_3$ as a solvent. The NMR chemical shifts are reported in ppm with reference to residual protons and carbons of $CDCl_3$ (δ 7.26 ppm in ^1H NMR, δ 77.0 ppm in ^{13}C NMR). Mass spectra (MS) were recorded on a Bruker Autoflex MALDI-TOF instrument using dithranol as a matrix.

Thermogravimetric analysis (TGA) was detected with a NETZSCH STA449 from 25°C to 600°C at a 20°C/min heating rate under N_2 atmosphere. To reveal the photophysical properties of emitters, UV-vis absorption spectra were measured by a SHIMADZU UV-1650PC. Steady-state photoluminescence (PL) spectra were obtained with a PTI QuantaMaster 40 steady-state fluorescence spectrofluorometer at room temperature. The luminescence lifetime, low temperature (77 K) fluorescence and phosphorescence spectra of the compounds in solution/film were measured with an Edinburgh FLS1000 transient-fluorescence spectrophotometer. Electrochemical property was evaluated by cyclic voltammetry with three typical electrodes in degassed CH_3CN solution with a rate of 100 mV/s in using a 273A (Princeton Applied Research). The CV system employed Bu_4NPF_6 as electrolyte. Platinum disk was used as the working electrode, platinum wire was regarded as the counter electrode and silver wire was used as the reference electrode. Ferrocenium/ferrocene

(Fc/Fc^{+}) was used as the external standard compound. Each oxidation potential was calibrated using ferrocene as a reference.

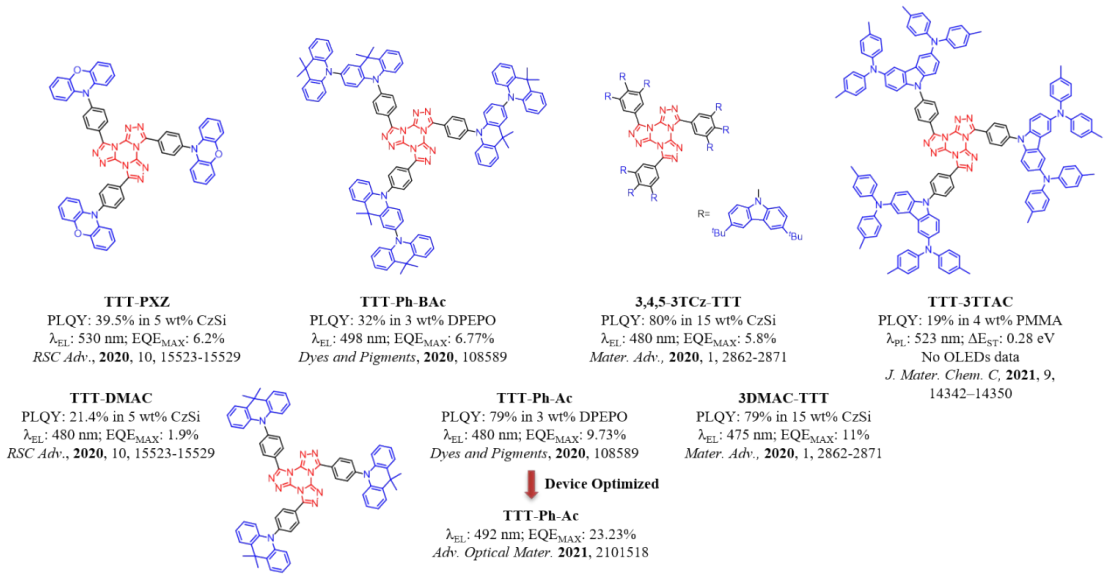

Figure S1. Chemical structures and performances of the reported TTT-based TADF emitters.

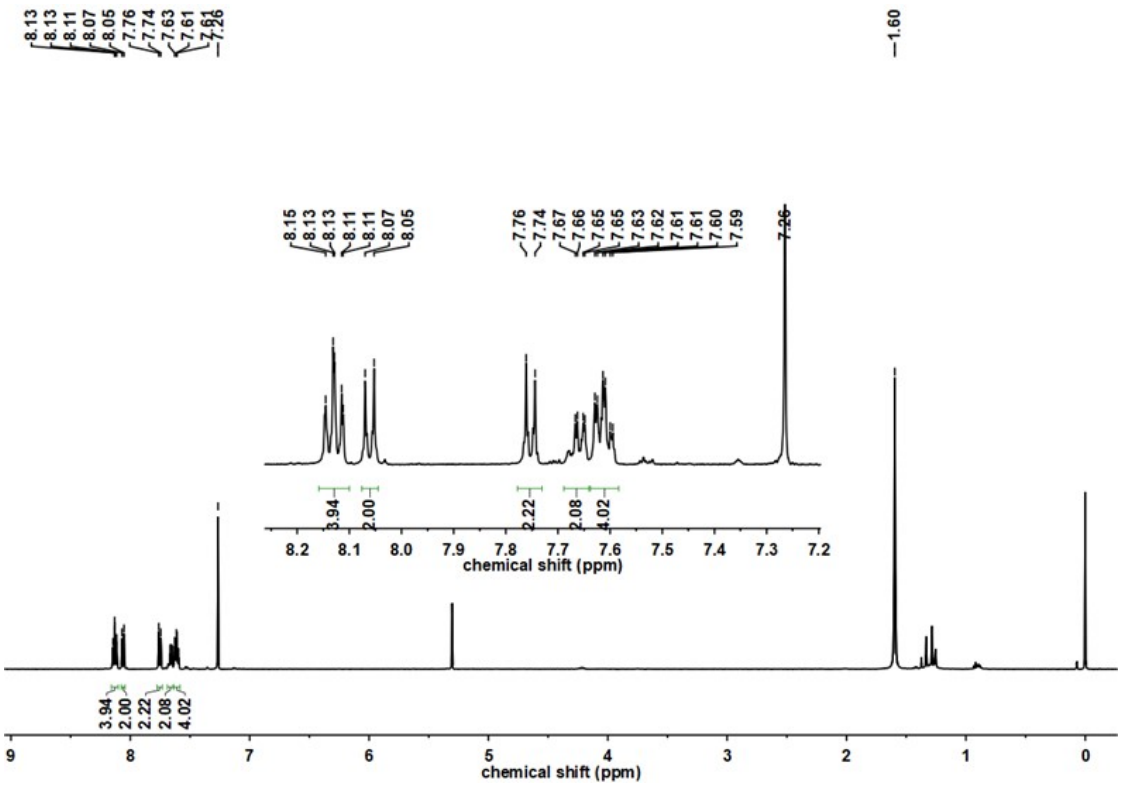

Figure S2. ^{1}H NMR spectrum of TTT-Br in $CDCl_3$.

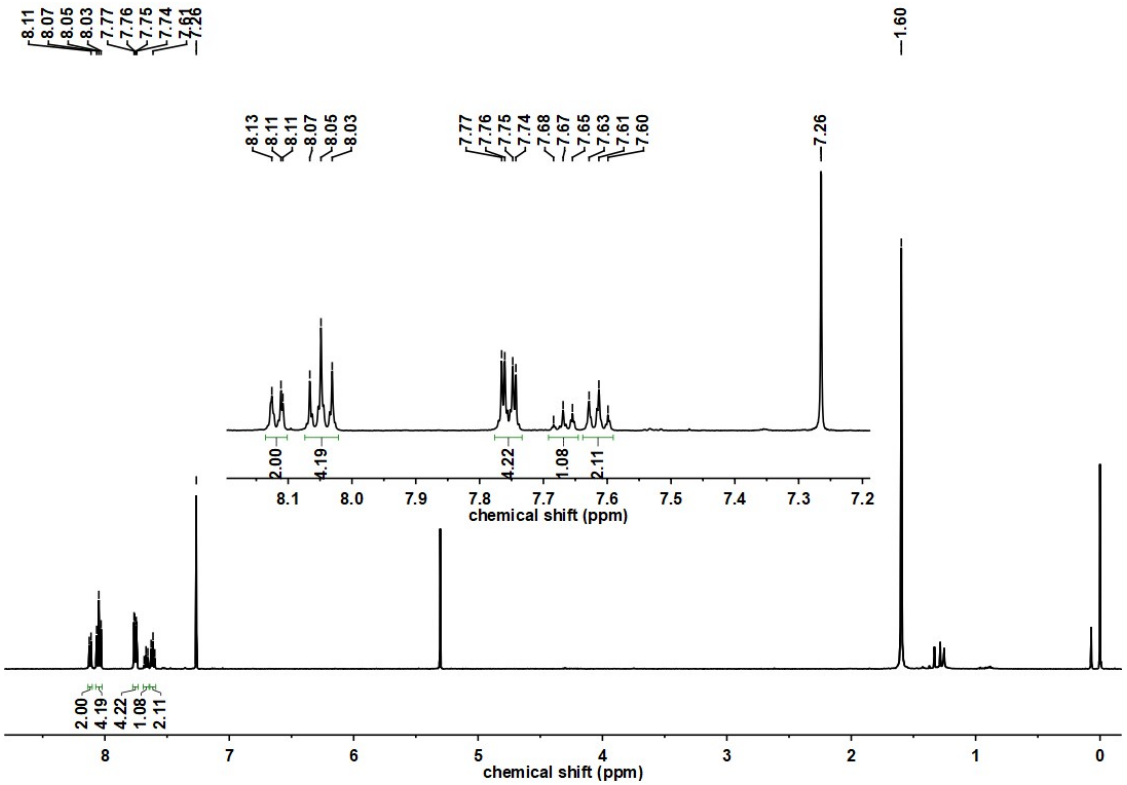

Figure S3. ^{1}H NMR spectrum of TTT-2Br in $CDCl_3$.

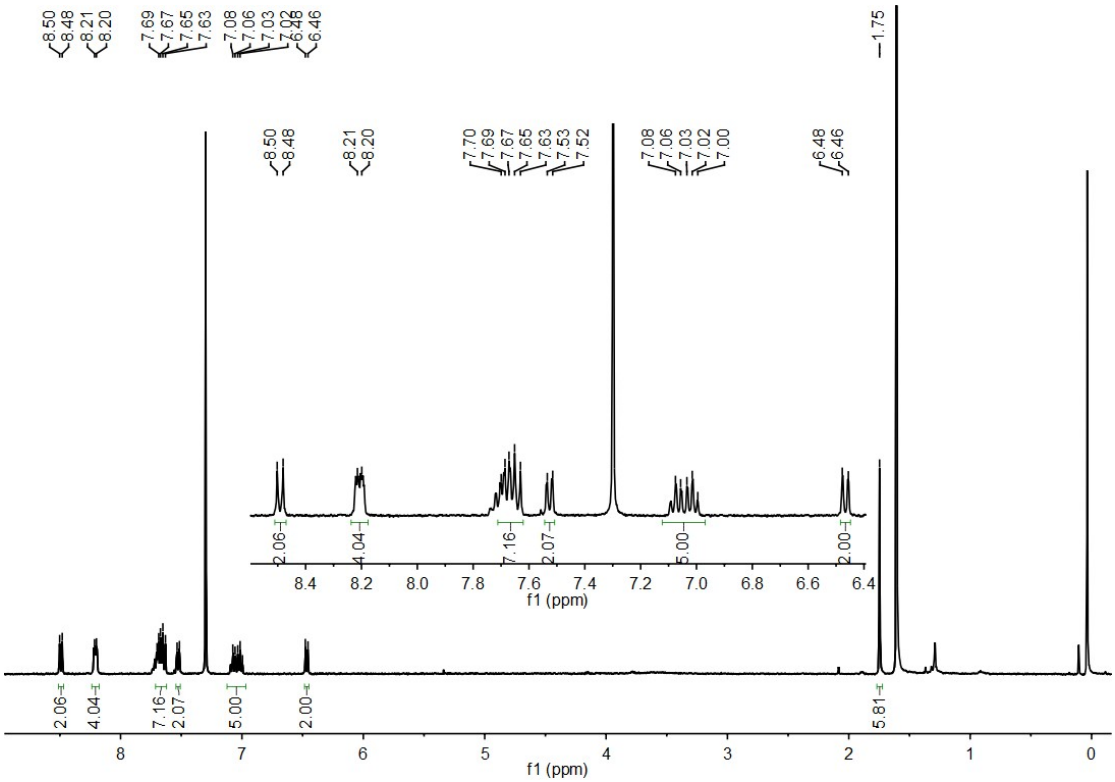

Figure S4. ^{1}H NMR spectrum of TTT-Ac in $CDCl_3$.

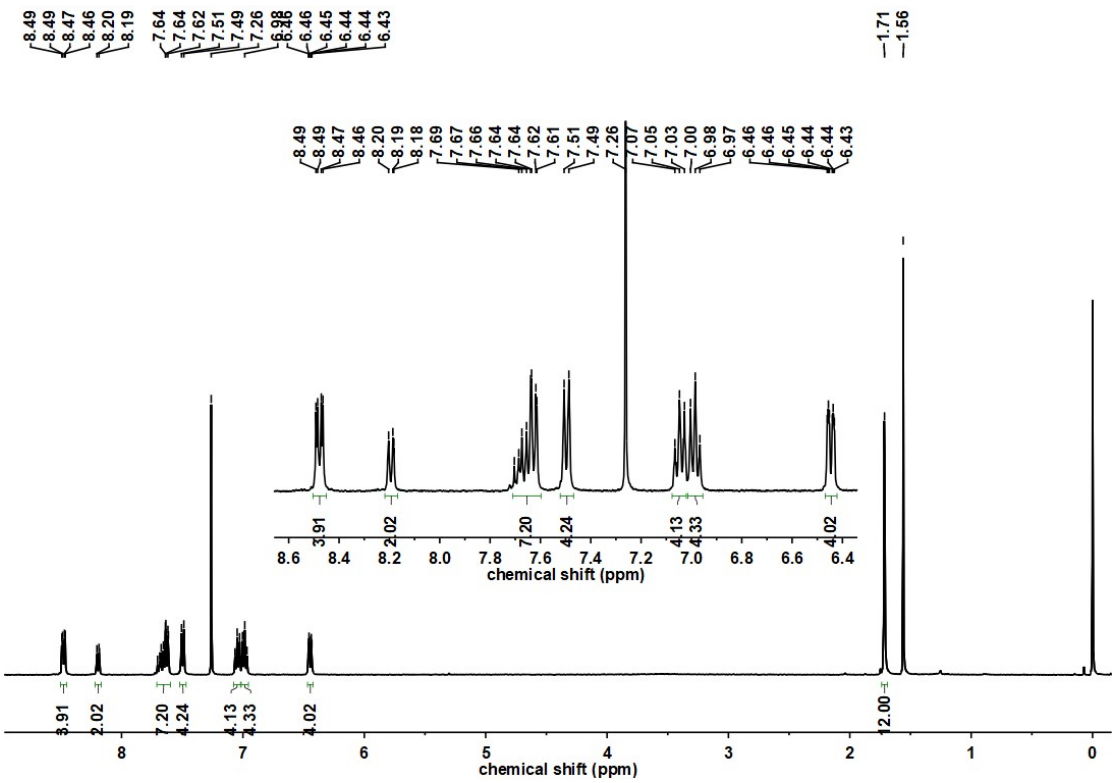

Figure S5. ^{1}H NMR spectrum of TTT-2Ac in $CDCl_3$.

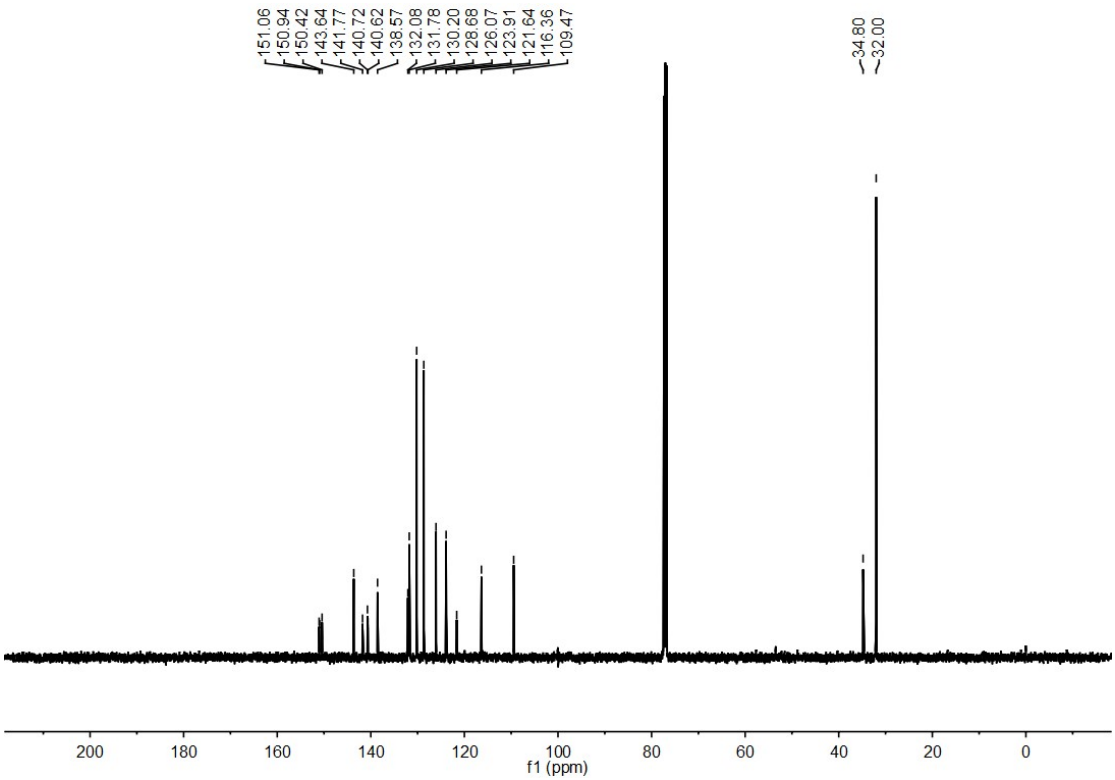

Figure S6. ^{13}C NMR spectrum of TTT-Ac in $CDCl_3$.

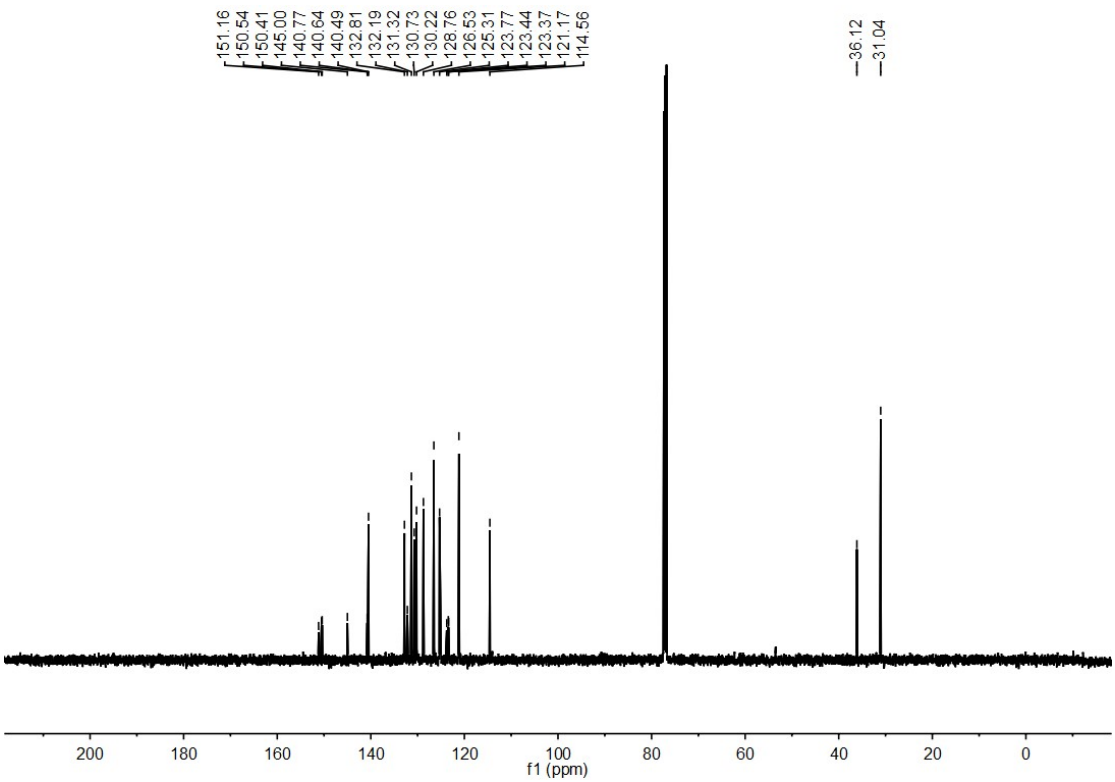

Figure S7. ^{13}C NMR spectrum of TTT-2Ac in $CDCl_3$.

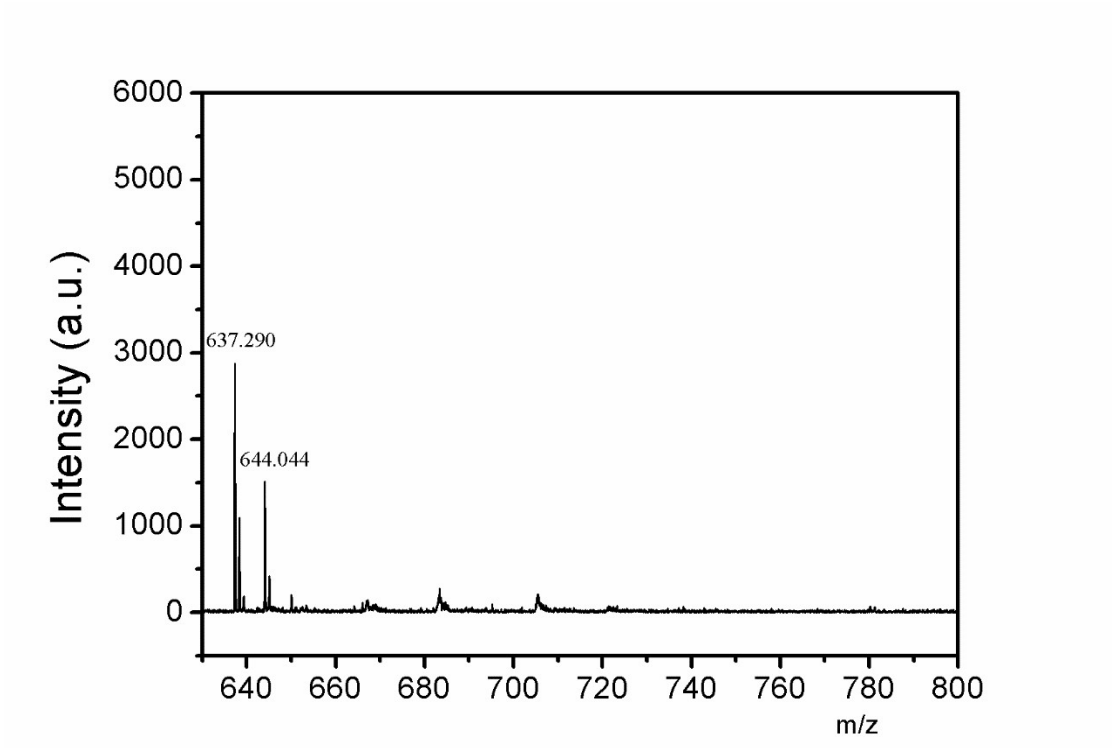

Figure S8. TOF-MS spectrum of TTT-Ac.

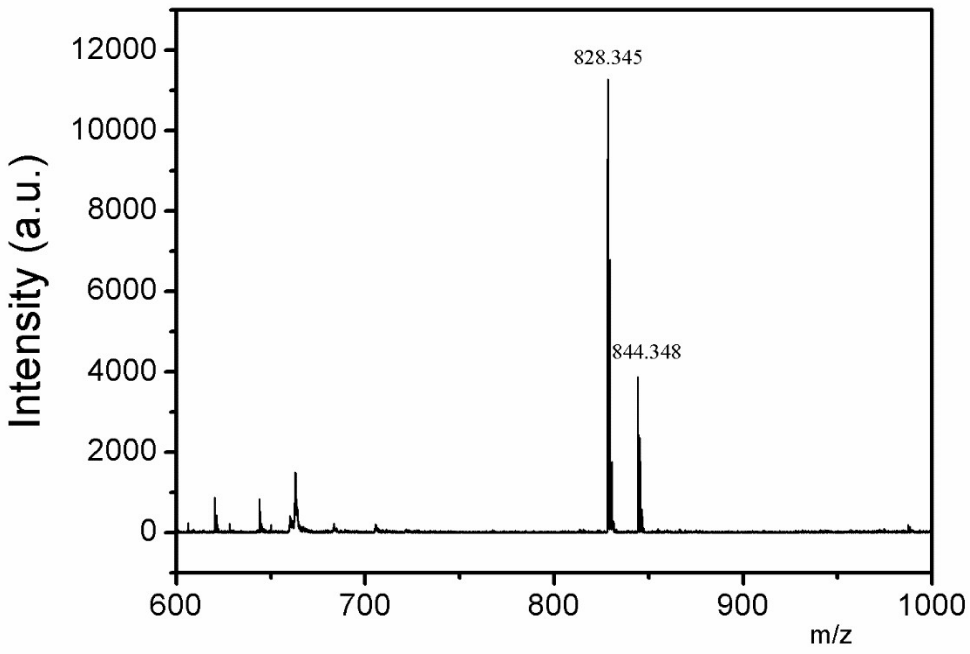

Figure S9. TOF-MS spectrum of TTT-2Ac.

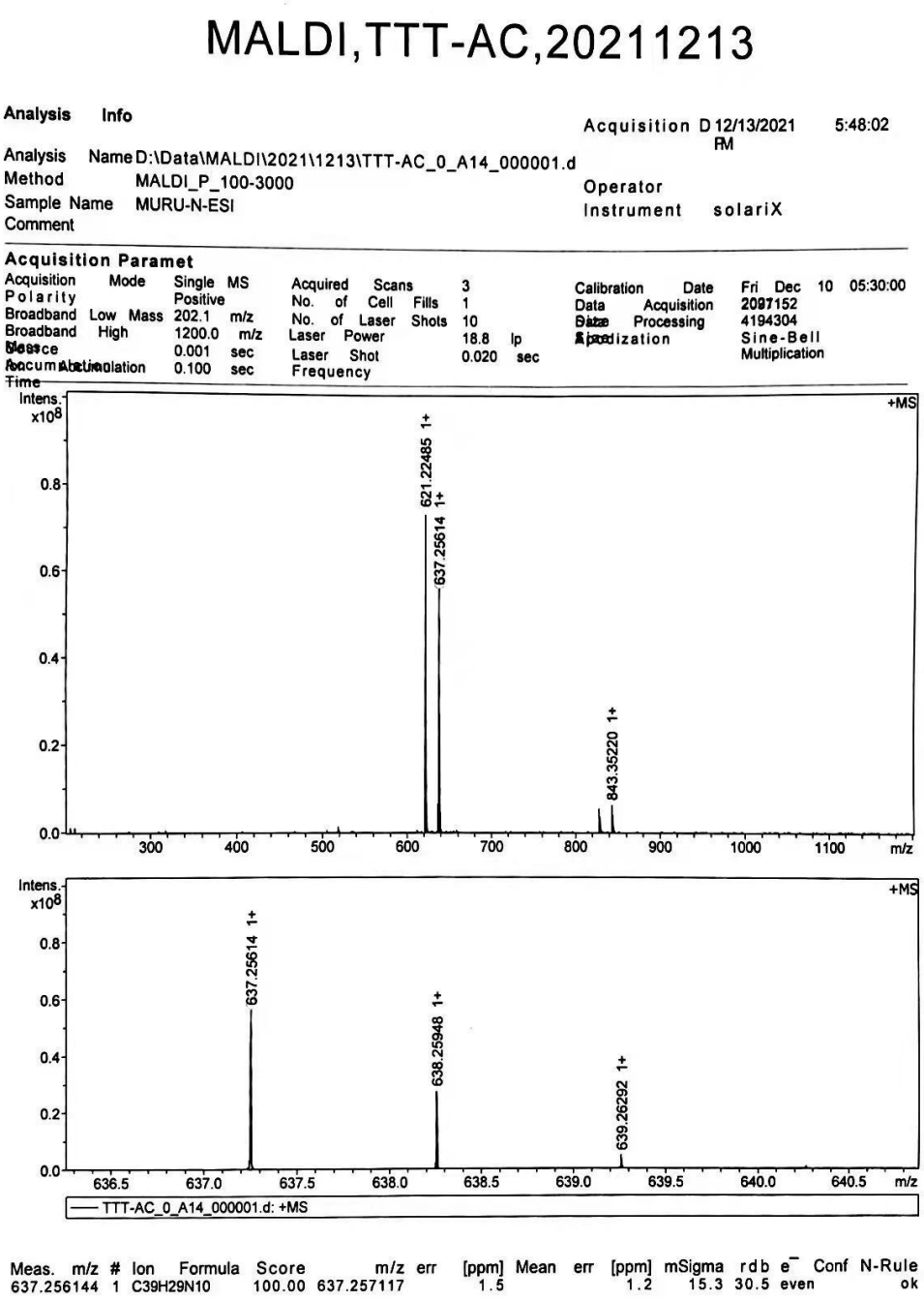

Figure S10. HRMS spectrum of TTT-Ac in CH_2Cl_2.

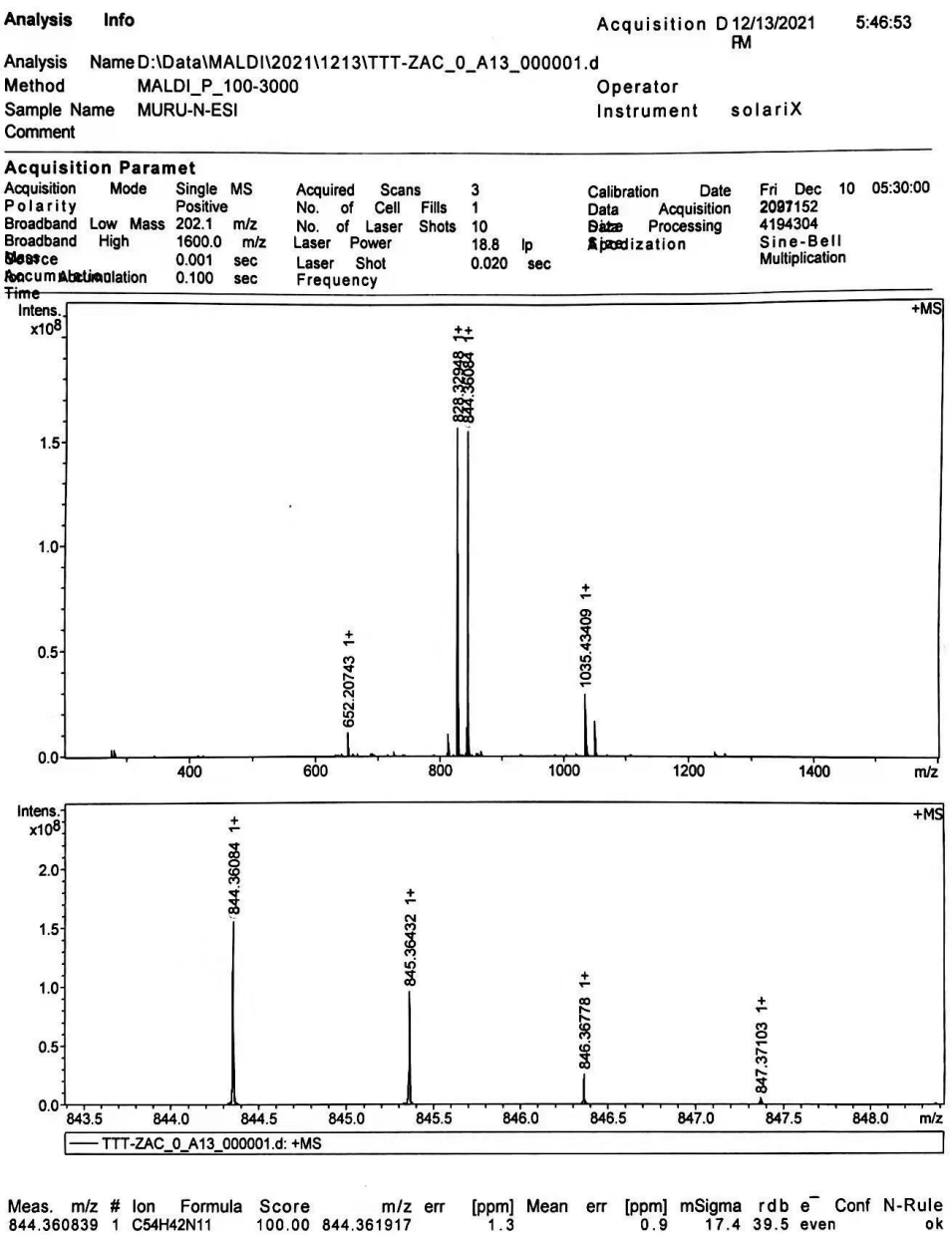

Figure S11. HRMS spectrum of TTT-2Ac in CH_2Cl_2.

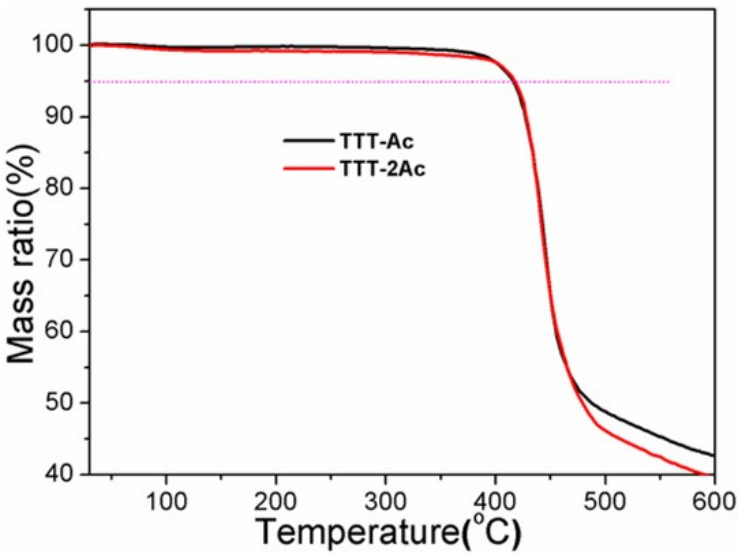

Figure S12. TGA curves of the compounds at N_2 atmosphere with a heating rate of 20°C min^{-1}.

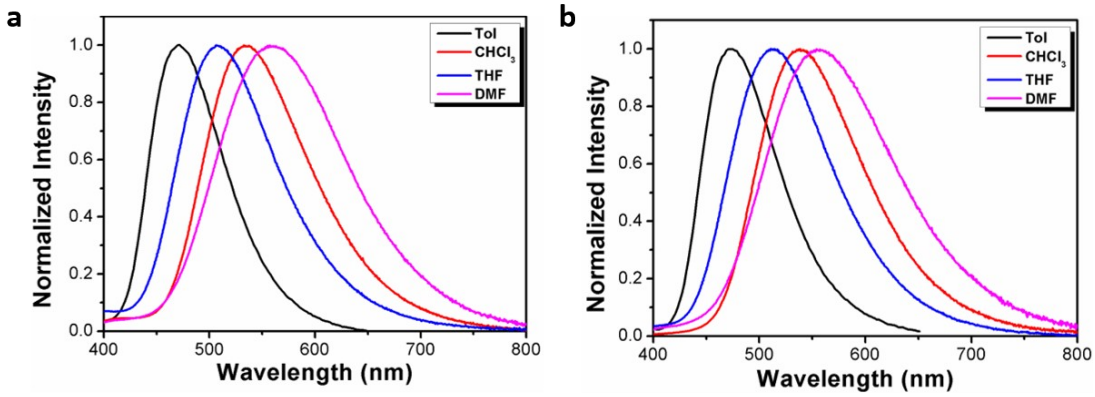

Figure S13. PL spectra of TTT-Ac (a) and TTT-2Ac (b) in different solvents at room temperature.

Table S1. Calculated Photophysical data of the TADF emitters.

Compound	τ_p/Φ_p (ns/%)	τ_d/Φ_d (μs/%)	k_p (10^7 s^{-1})	k_d (10^4 s^{-1})	k_{ISC} (10^7 s^{-1})	k_{rISC} (10^4 s^{-1})	k_r ($10^7 s^{-1}$)	k_{nr} (10^4 s^{-1})
TTT-Ac	10.9/21	27.2/42	9.17	3.68	7.24	9.32	1.93	1.72
TTT-2Ac	11.9/10	20/37	8.4	5	7.56	20.55	0.84	2.95

$k_p = 1/\tau_p$ (1)

$k_d = 1/\tau_d$ (2)

$k_{ISC} = (1-\Phi_p)k_p$ (3)

$k_{rISC} = k_p k_d \Phi_d / k_{ISC} \Phi_p$ (4)

$k_r = \Phi_p/\tau_p$ (5)

$k_{nr} = k_d - \Phi_p k_{rISC}$ (6)

Herein, τ_p and τ_d are the lifetime of prompt and delayed components. Φ_p and Φ_d are the prompt and delayed luminescence quantum efficiency, respectively. The k_p and k_d are the rate constant of prompt and delayed fluorescence. k_{ISC} is the rate constant of intersystem crossing, while k_{rISC} is the rate constant of reverse intersystem crossing between the S_1 and T_1. k_r and k_{nr} are the radiative and nonradiative decay rate constant from S_1 to S_0, respectively.

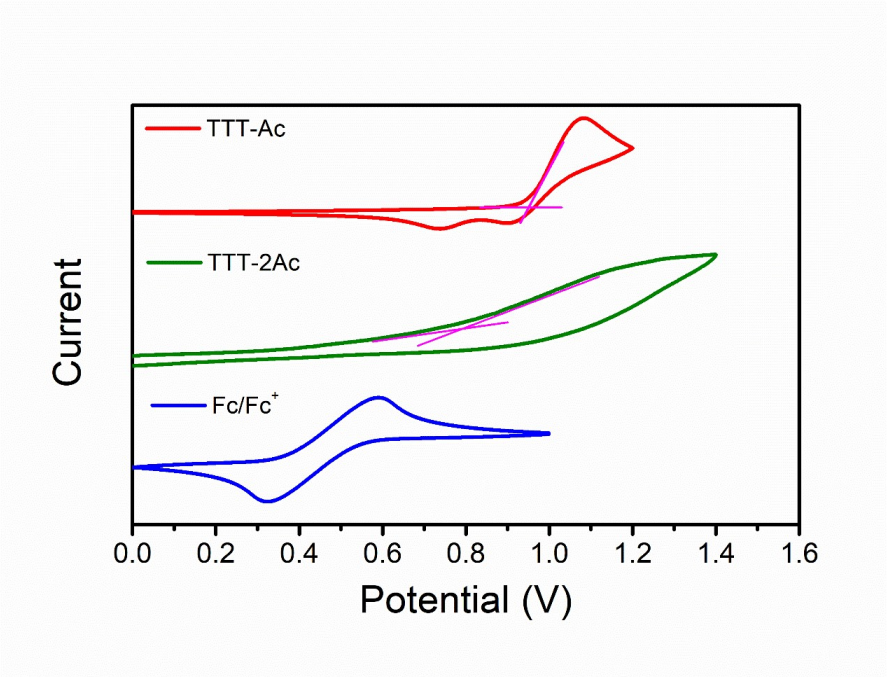

Figure S14. CV curves of compounds in CH_3CN solution.

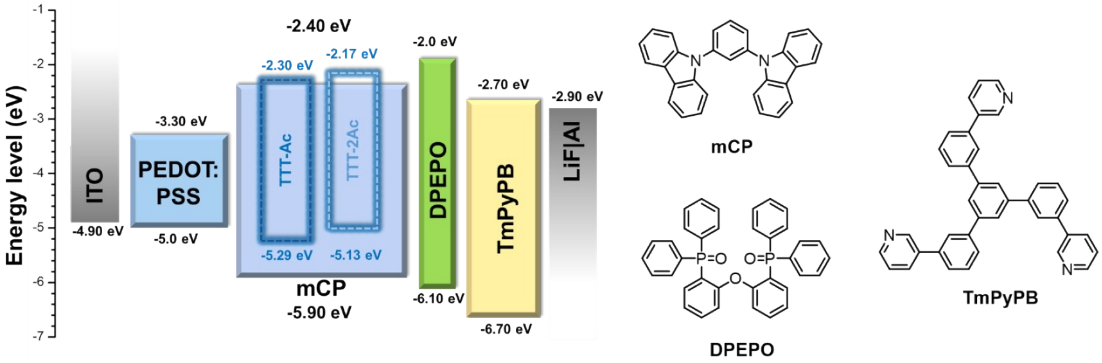

Figure S15. The energy level diagrams and chemical structures of the materials in the devices.

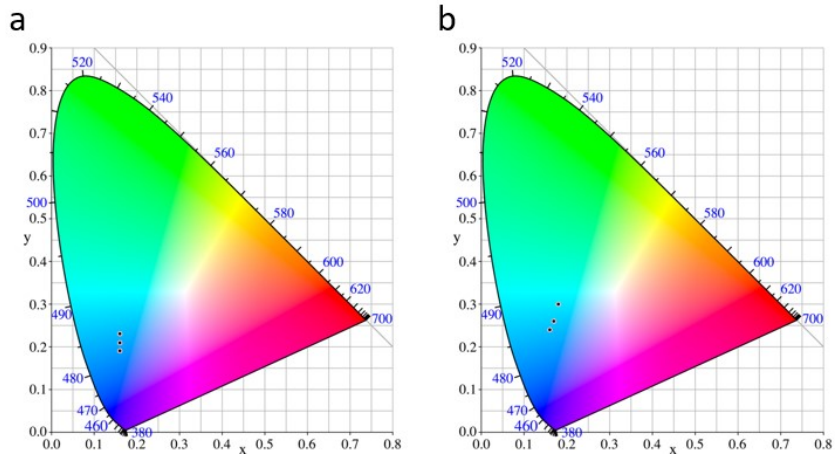

Figure S16. CIE coordinates of the devices: (a): TTT-Ac; (b) TTT-2Ac.

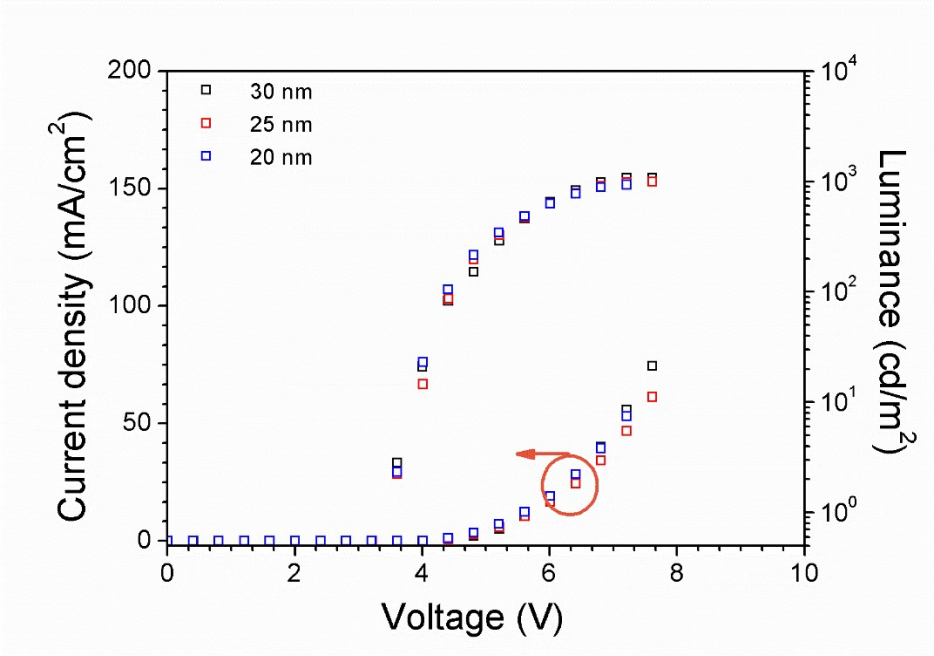

Figure S17. Current density-voltage-luminance (J-V-L) curves (c) of TTT-Ac with different EML thickness of 20 wt% dopants.

Table S2. EL data for the devices with different EML thickness.

Material	EML Thickness (nm)	Dopant wt%	V_{ON} V	L_{max} cd m^{-2}	CE_{max} cd A^{-1}	EQE_{max} %	CIE (x, y)	Peak nm
TTT-Ac	30	20%	3.6	1078	16.21	9.26	(0.16，0.21)	470
	25	20%	3.6	996.4	17.37	10.01	(0.16，0.22)	474
	20	20%	3.6	935.3	14.52	8.48	(0.16，0.23)	470

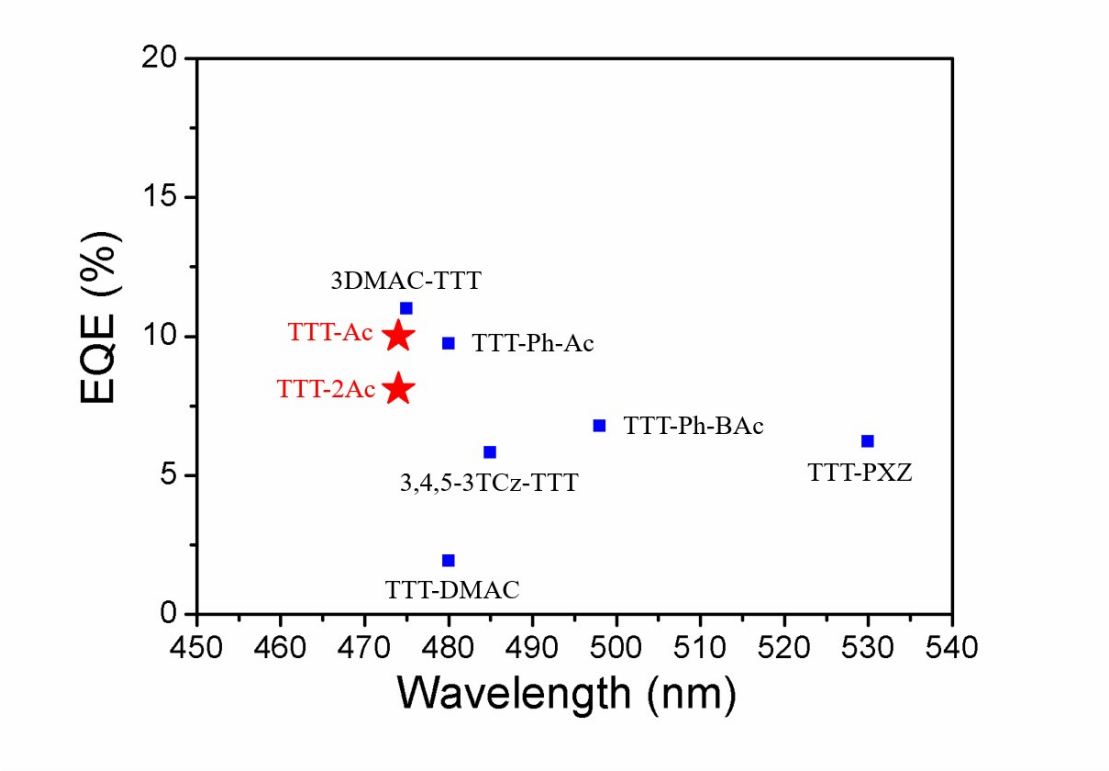

Figure S18. EQE-wavelength curves of the TTT-based TADF emitter.